# Advanced Algorithms for Pseudo-Range Estimation and Positioning Accuracy in Challenging Satellite Visibility Conditions

P. Sirish Kumar [1,*], A. Jayalaxmi[1], V. B. S. Srilatha Indira Dutt [2], P. Krishna Rao [1], P. Kameswara Rao [1], and L. Ganesh [3]

[1] Department of Electronics and Communication Engineering, Aditya Institute of Technology and Management, Tekkali, Andhra Pradesh, India
[2] Department of Electronics and Communication Engineering, GITAM University (deemed to be University), Visakhapatnam, Andhra Pradesh, India
[3] Department of Electronics and Communication Engineering, Gayatri Vidya Parishad College of Engineering for Women, Visakhapatnam, India
Email: sirishdg@gmail.com (P.S.K.); jayalaxmi.anem@gmail.com (A.J.); srilatha06.vemuri@gmail.com (V.B.S.S.I.D.); pkr.aitam@gmail.com (P.K.R.); kameshpedada@gmail.com (P.K.R.); ganeshlaveti2010@gmail.com (L.G.);
*Corresponding author

***Abstract*—Accurate Global Positioning System (GPS) positioning is critical for numerous applications, yet traditional navigation algorithms such as Gradient Descent (GD), Least Squares (LS), and Weighted Least Squares (WLS) often face challenges in terms of convergence speed, computational complexity, and robustness, especially under conditions of low satellite visibility. This paper proposes a new navigation solution, the Levenberg (LVB) algorithm, designed to address these challenges. The LVB algorithm integrates the strengths of GD and LS, using an adaptive learning coefficient to provide optimal estimates without encountering the inverse problems associated with LS. We evaluated the performance of LVB alongside GD, LS, and WLS using real GPS receiver data collected from the Indian Institute of Science (IISc) in Bangalore. Our results demonstrate that LVB outperforms the traditional methods, delivering more accurate and reliable GPS position estimates, particularly in scenarios with limited satellite visibility, which is beneficial for users in the Indian subcontinent.**

***Keywords*—gradient descent, least squares, levenberg, pseudo-range, time or arrival, weighted least squares**

## I. Introduction

Currently, ground-based navigational aids remain the dominant navigation mode for air traffic services worldwide, while Global Navigation Satellite System (GNSS) functions as the backup system. Each airport uses distinct frequencies for their navigational signals, but these systems have limited accuracy, such as Doppler Very high frequency Omnidirectional Range (DVOR) accuracy being approximately 90 m at ±2 nmi. Issues related to interoperability and multipath effects further compound their challenges. The ground-based navigational aids offer a horizontal accuracy of 10m and vertical accuracy of 5 m. Consequently, the International Civil Aviation Organization (ICAO) has proposed to rely on existing GNSS for more precise air traffic services, particularly to address the growing congestion in air traffic [1]. According to the proposed plan, GNSS is positioning itself to take on the primary role in navigation, while ground-based navigation will assume a secondary role shortly. GNSS encompasses multiple global constellations, such as GPS, Europe's global navigation satellite system (Galileo), Russian satellite navigation system (GLONASS), and BeiDou. GPS is the sole fully operational global constellation boasting 32 satellites, efficiently transmitting signals across five distinct frequencies. This extensive satellite coverage guarantees visibility of 14 to 18 satellites from any point on Earth's surface, endowing GNSS with exceptional reliability and robustness as a navigation solution. These advancements position GNSS as an ideal fit for addressing the evolving needs of modern air traffic management, ensuring safer and more efficient global navigation for aircraft.

The introduction of GPS has revolutionized navigation, particularly in civil aviation. Satellite-based navigation systems generally provide higher accuracy compared to traditional aids, but the precision of positional readings can be affected by several error factors. These factors encompass ionospheric and tropospheric delays, satellite clock biases, receiver quality, multi-path effects, and the spatial relationship between the receiver and satellites. Consequently, standalone GPS needs to meet the stringent requirements for aircraft landing, particularly for Category-I (CAT-I) precision approaches. Such

Manuscript received April 3, 2024; revised July 22, 2024; accepted August 2, 2024; published October 10, 2024.

approaches mandate horizontal and vertical accuracies of 16 meters and 4.5–7 meters, respectively. Hence, a critical need arises to elevate GPS performance, which can be achieved through augmentation techniques like Space-Based Augmentation Systems (SBAS). SBAS fulfills enroute navigation accuracy standards, including an accuracy of 2.2 nautical miles and an integrity of 2 minutes.

Moreover, it provides vertical guidance with a horizontal accuracy of 220 meters, vertical accuracy of 20 meters, and an integrity of 10 seconds [2]. By adopting Satellite Based Augmentation System (SBAS), the aviation industry strives to bolster GPS performance significantly, ensuring the precision, reliability, and safety required for seamless and efficient air travel. As technology evolves, the integration of SBAS with GPS promises to bring about further advancements in air navigation, catering to the ever-increasing demands of modern aviation.

This study introduces the Levenberg (LVB) algorithm, designed to enhance GPS positioning accuracy and robustness. By comparing LVB with traditional algorithms such as Gradient Descent with Armijo, Least Squares, and Weighted Least Squares, we demonstrate its superior performance using real GPS data from Bangalore, India. Our analysis shows that LVB significantly reduces positional errors and uncertainties, especially in scenarios with limited satellite visibility. These findings highlight the practical benefits of LVB for improving GPS accuracy in the Indian subcontinent.

## II. Literature Review

To achieve the objectives of this paper, a comprehensive understanding of positioning systems is crucial. This includes concepts and system details of source localization, the Global Positioning System (GPS), measurement techniques, GPS signal structure, and GPS observables. Iterative and recursive navigation algorithms and knowledge of linear algebra are also essential components. Approximately 13.3% of recent scientific publications focusing on positioning highlight the significance of object tracking and localization [3]. Research in positioning systems mainly revolves around two vital areas: localizing radiating sources within the system's coverage area and globally positioning unknown objects [4]. Source localization systems have gained widespread use due to their compact size and low power consumption. They find applications in various domains, such as civil and military applications for field surveying, capsule endoscopy, inventory control, soldier and mine tracking, and intelligence gathering [5]. Moreover, the global positioning of unknown objects assumes paramount significance in civil aviation and the defense sector, enabling essential functionalities such as precise aircraft landings and accurate ship navigation [6]. The literature abounds with a wide array of vital applications of positioning systems, highlighting the escalating need and demand for these cutting-edge technologies [7]. As positioning systems advance rapidly, their crucial role in various industries becomes more evident. From enhancing logistics and transportation to optimizing precision agriculture and supporting emergency response systems, positioning technologies profoundly impact our modern world. As we embrace further innovations and explore new frontiers in satellite-based positioning, the scope of its applications is expected to expand even further, catalyzing advancements across multiple sectors and redefining the way we navigate and interact with our environment.

The source localization system necessitates the deployment of a group of receivers in the surveyed area. These receivers are designed to receive and track radio signals emitted by the unknown source, which are measurements [8]. Notably, the exact locations of these receivers are often unknown at the time of deployment. Additionally, these receivers can be mobile if necessary for added flexibility and adaptability. Therefore, the localization of individual receivers is also important [9] and therefore requires an optimal measurement technique and positioning algorithm. Various techniques are evolved for collecting these measurements from the unknown source and are based on the type of source, type of operating medium and environmental conditions. The techniques Time of Arrival (TOA), Time Difference of Arrival (TDOA), Received Signal Strength (RSS) and Direction of Arrival (DOA) used to collect measurements, their implementation, system constraints, fundamental operation and limitations are well understood [10, 11].

Moreover, the integration of multi-frequency and multi-GNSS systems has significantly improved the precision and reliability of positioning solutions [12]. Techniques such as Precise Point Positioning (PPP) and Real-Time Kinematic (RTK) positioning are now widely used to achieve centimeter-level accuracy in various applications, including autonomous vehicles and high-precision agriculture [13]. The development of novel algorithms for error mitigation, such as those addressing multipath effects and ionospheric delays, has also contributed to the advancement of positioning technologies [14]. These innovations enhance the resilience of positioning systems in challenging environments, further expanding their applicability and effectiveness.

## III. Materials and Methods

A This section presents a comprehensive outline of the procedures involved in implementing different existing navigation solutions, namely the Least Squares (LS), Weighted Least Squares (WLS), and Gradient Descent with the Armijo (GD) algorithm. Subsequently, the detailed implementation of the proposed navigation algorithm, the Levenberg (LVB) algorithm, is presented.

### *A. Objective Function Determination*

These algorithms (LS, WLS, GD, LVB) are iterative techniques employed to address the over-determined navigation problem, where the objective function is formulated as the sum of squared differences [15]. When applied to the three-point GPS problem in an over-determined scenario, the objective function 'obj' is represented as follows:

$$obj\left(Pr_i, \vec{U}\right) = \frac{1}{2} \times \sum_{i=1}^{m} \left(Pr_i - \sqrt{(x_i - x_u)^2 + (y_i - y_u)^2 + (z_i - z_u)^2}\right)^2$$

$$= \frac{1}{2} \times \sum_{i=1}^{m} \left( Pr_i - f(\vec{U}) \right)^2 \quad (1)$$

Eq. (1) can be alternatively expressed as:

$$obj(Pr_i, \vec{U}) = \frac{1}{2} \times \sum_{i=1}^{m} (r_i)^2 \quad (2)$$

where, $r_i$= Measurement residual

The primary goal is to determine the minimum value of the multi-variable objective function defined in Eq. (1) concerning to $\vec{U} = [x_u, y_u, z_u]^T$, thereby yielding the estimation of the receiver position vector $\vec{U} \cong \vec{U}_K = [x_{uK}, \ y_{uK}, \ z_{uK}]^T$. In order to facilitate the computation of derivatives, the function presented in Eq. (1) is scaled by a factor of 0.5, simplifying the optimization process.

### *B. Least Squares Algorithm*

The three-point GPS navigation problem in the over-determined case is classified as a non-linear least squares problem [16]. The task involves solving Eq. (1) to determine the minimum value with respect to the unknown variable $\vec{U}$, as depicted below:

$$\arg\min_{\vec{U}} (\text{obj}(\text{Pr}_i, \vec{U})) \quad (3)$$

Recalling Eq. (1) and Eq. (2), the residual vector can be given as:

$$r_i = Pr_i - f(\vec{U}) \quad (4)$$

We must equate its gradient to zero to find the minimum value of the objective function 'obj' in Eq. (3). This critical point represents the optimal solution where the function reaches its lowest point, providing valuable insights into the problem.

$$\nabla obj = \frac{\partial obj(Pr_i, \vec{U})}{\partial \vec{U}} = 0$$

Given that the model encompasses three parameters, represented as $\vec{U} = [x_u, y_u, z_u]^T$, we create three gradient equations. The gradient for Eq. (3) is formulated as follows:

$$\frac{\partial obj(Pr_i, \vec{U})}{\partial \vec{U}} = \sum_{i=1}^{m} r_i \frac{\partial r_i}{\partial \vec{U}} = 0 \quad (5)$$

The derivative in Eq. (5) is represented as:

$$\left. \frac{\partial obj(Pr_i, \vec{U})}{\partial \vec{U}} \right|_{\vec{U}=\vec{U}_K} = \left( -\sum_{i=1}^{m} J_{ji}^T \times r_i \right)_{\vec{U}=\vec{U}_K} = 0 \quad (6)$$

here, 'j' represents the number of unknown parameters or the size of vector $\vec{U}$. During each iteration, the function $f(\vec{U})$ is linearized with respect to $\vec{U} = \vec{U}_K$ and the unknown parameter is $\delta\vec{U}$ defined as in Eq. (7), which is subsequently utilized for successive updates to the receiver position vector u $\vec{U}_K$.

$$\delta\vec{U} = (J^T J)^{-1} J^T \delta\vec{P}r \quad (7)$$

here, in Eq. (7) the term, $J^T J$ represents approximated Hessian matrix, 'Hess'.

- *Step-by-Step Computation of Navigation Solution using Least Squares Method*

Step 1. Using '*m*' satellites, collect pseudo-range measurements *Pr*1, *Pr*2, ..., *Prm*.

Step 2. Receiver position vector $\vec{U}_k = [x_{uK}, y_{uK}, z_{uK}]^T$ is initialized to 0 (i.e. *K*=0).

Step 3. Based on the receiver position in step 2, calculate the range measurements, $\text{Pr}_{1K}$, $\text{Pr}_{2K}$, …, $\text{Pr}_{mK}$

Step 4. Determine the Jacobian matrix, $J_{m\times 3}$.

Step 5. Take the measurement vector $\delta\vec{P}r = [\delta\text{Pr}_1 \quad \delta\text{Pr}_2 \quad ... \text{Pr}_m]^T$ and calculate the error from steps 1 and 3.

Step 6. Using Eq. (7), determine the update value or change in position $\delta\vec{U} = [\delta x_u \quad \delta y_u \quad \delta z_u]^T$

Step 7. Using the position vector obtained in Step 6, update the receiver position vector in Step 2. (i.e. $\vec{U}_{K+1} = \vec{U}_K + \delta\vec{U}$)

Step 8. Carry out iterations of Steps 3–7 either for a predetermined number of cycles or until the predefined threshold condition is satisfied. (like $\sqrt{(\delta x_u)^2 + (\delta y_u)^2 + (\delta z_u)^2} \leq threshold$).

Step 9. $\vec{U}_{K+1} = [x_{uK+1}, y_{uK+1}, z_{uK+1}]^T$ is the final estimate of the receiver position.

### *C. Weighted Least Squares Algorithm*

The least squares solutions for the GPS three-point navigation problem with the over-determined case discussed so far assume that the error in the pseudo-range measurements observed at the receiver has a constant variance and consider their effect equally in estimating the receiver position [17]. In practice, the separation in distance between satellite-satellite and satellite-receiver is different, and the uncertainty in the observed measurement varies with distance. With the increase in distance, the time a signal travels in the atmosphere increases and possibly gets affected more in ionospheric and tropospheric layers. In addition, the elevation angle, geographical conditions etc., also lead to variable uncertainty and error variance in observed measurements.

Accordingly, the weighted least squares criterion minimized to obtain the receiver position estimates is modified from Eq. (1) and is given as follows.

$$obj(Pr_i, \vec{U}, w_i) = \frac{1}{2} \times \sum_{i=1}^{m} w_i \times \left( Pr_i - f(\vec{U}) \right)^2 \quad (8)$$

here, $w_i$ is the weight coefficient of i[th] pseudo-range measurement which is a constant and is computed from variance-covariance matrix. The measurement error, $\delta \text{Pr}_i$ (with $i$ = 1 ,2, ..., $m$) in receiver position estimation given

in Eq. (7) is used in designing the variance matrix. The process of linearization and successive approximation of the receiver position follows a similar procedure as in LS with the position update equation as given below.

$$\delta\vec{U} = (J^T wJ)^{-1} J^T w\left(\delta\vec{P}r\right) \quad (9)$$

The matrix given in Eq. (9) is one method of determining the weight matrix, and the efficiency of the WLS position estimation algorithm depends entirely on the weight matrix design method [18]. This article uses the above matrix to implement the WLS navigation algorithm.

- *Step-by-Step Computation of Navigation Solution using Weighted Least Squares*

Step 1. Collect the observed pseudo-range measurements $Pr_1$, $Pr_2$, …, $Pr_m$.

Step 2. Initialize the receiver position vector, $\vec{U}_k = [x_{uK}, y_{uK}, z_{uK}]^T$ (i.e. K = 0).

Step 3. Compute the range measurements, $\mathrm{Pr}_{1K}$, $\mathrm{Pr}_{2K}$, …, $\mathrm{Pr}_{mK}$ using the receiver position in step 2.

Step 4. Calculate the error in measurement vector, $\delta\vec{\mathrm{P}}\mathrm{r} = [\delta\mathrm{Pr}_1 \quad \delta\mathrm{Pr}_2 \quad \ldots \quad \mathrm{Pr}_m]^T$ from steps 1 and 3.

Step 5. Compute the weights based on the measurement error obtained in step 4.

Step 6. Calculate the Jacobian matrix, $J_{m\times 3}$.

Step 7. Determine the update value or change in position $\delta\vec{U} = [\delta x_u \quad \delta y_u \quad \delta z_u]^T$ with Eq. (9).

Step 8. Using the position vector obtained in Step 7, update the receiver position vector in Step 2. (i.e. $\vec{U}_{K+1} = \vec{U}_K + \delta\vec{U}$)

Step 9. Carry out iterations of Steps 3–8 either for a predetermined number of cycles or until the predefined threshold condition is satisfied. (like $\sqrt{(\delta x_u)^2 + (\delta y_u)^2 + (\delta z_u)^2} \leq threshold$).

Step 10. $\vec{U}_{K+1} = [x_{uK+1}, y_{uK+1}, z_{uK+1}]^T$ is the final estimate of the receiver position.

### D. Gradient Descent with Armijo

The Gradient Descent algorithm is an iterative method that employs a line search strategy to solve Eq. (1). At each iteration (denoted by K), the algorithm selects a direction, $p_K$, and then explores along this direction to find a lower function value. In this process, the algorithm determines the new state vector estimates for the current iteration K, represented by vector $\vec{U}_K = [x_{uK}, y_{uK}, z_{uK}]^T$, and utilizes this information to update the state vector estimates for the next iteration, given by:

$$\vec{U}_{K+1} = \vec{U}_K + \alpha_K p_K \quad (10)$$

To minimize the function, the direction opposite to the gradient is used and following a specific step length criterion, the receiver position vector is updated which is given as:

$$\vec{U}_{K+1} = \vec{U}_K + \alpha_K(-\nabla obj) \quad (11)$$

The gradient, $\nabla$ of the function, 'obj' can be calculated as [13],

$$\nabla obj(Pr_i, \vec{U}) = \sum_{i=1}^{m} r_i \frac{\partial r_i}{\partial \vec{U}}|_{\vec{U}=\vec{U}_K} = (-J^T_{3\times m} \times \vec{r})_{\vec{U}=\vec{U}_K} \quad (12)$$

From Eq. (11), Eq. (12) can be updated as:

$$\vec{U}_{K+1} = \vec{U}_K + \alpha_K(J^T_{3\times m} \times \vec{r})_{\vec{U}=\vec{U}_K} \quad (13)$$

As mentioned previously, along with the direction, $p_K$, the choice of step length, $\alpha_K$ is also important and this algorithm makes use of Armijo criterion in choosing the step length, which is given as [19]:

$$obj\left(Pr_i, \vec{U}_{K+1}\right) \leq obj\left(Pr_i, \vec{U}_K\right) - c_1\alpha_K \nabla obj(Pr_i, \vec{U}_K)^T \nabla obj(Pr_i, \vec{U}_K) \quad (14)$$

where, $c_1$ is some small scalar constant.

- *Step-by-Step Computation of Navigation Solution using the GD-Armijo Method*

Step 1. Initialize the values for the variables: step length $\alpha_K$, the constant parameter $c_1$ and the apriori receiver position vector estimate $\vec{U}_K$.

Step 2. Using '$m$' satellites, collect pseudo-range measurements $Pr_i$ with $I$ = 1, 2, 3, …, $m$

Step 3. Calculate the pseudo-range measurements, $\vec{\mathrm{Pr}}_{\mathrm{iK}}$ with the position vector $\vec{U}_K$.

Step 4. Determine the error in the measurement vector, $\vec{\mathrm{r}} = \delta\vec{\mathrm{P}}\mathrm{r} = \mathrm{Pr}_i - \mathrm{Pr}_{\mathrm{iK}}$.

Step 5. Evaluate the objective function, $e_0 = obj\left(Pr_i, \vec{U}_K\right)$ and compute the Jacobian matrix, J.

Step 6. Update the receiver position vector estimate in step 1.($\vec{U}_{K+1} = \vec{U}_K + \alpha_K(J^T \times \vec{r})$)

Step 7. Compute the pseudo-range measurement, $Pr_{iK+1}$ with the new update of $\vec{U}_{K+1}$ in step 6.

Step 8. Determine the error in measurement vector, $\vec{\mathrm{r}} = \delta\vec{\mathrm{P}}\mathrm{r} = \mathrm{Pr}_i - \mathrm{Pr}_{\mathrm{iK}+1}$.

Step 9. Evaluate the objective function, $e_1 = obj\left(Pr_i, \vec{U}_{K+1}\right)$

Step 10. With $e_0$, $e_1$, $c_1$ and $\alpha_K$ check for Armijo criterion in Eq. (14)

Step 11. If the criterion is satisfied increase the step size by $\alpha_K = \alpha_K \times 10$ and repeat the steps 6 to 10.

Step 12. If the criterion fails, Decrease the step size i.e. $\alpha_K = \alpha_K/10$, compute $\vec{U}_{K+1} = \vec{U}_K + \alpha_K(J^T \times \vec{r})$ and repeat the steps from 3 to 10, till the objective function value reaches a predefined threshold value.

Step 13. $\vec{U}_{K+1} = [x_{uK+1}, y_{uK+1}, z_{uK+1}]^T$ is the final estimate of the receiver position.

### E. Levenberg Algorithm

In addition to the Gradient Descent navigation solution, the remaining two algorithms necessitate the computation of the inverse of the approximated Hessian matrix, denoted

as Hess ≅ $J^T J$ [20], as shown in Eq. (7) and Eq. (9). Nevertheless, in situations involving intricate error space optimization, the matrix Hess may not be invertible. To address this, the Levenberg algorithm introduces an additional approximation to the Hessian matrix, ensuring its invertibility.

$$Hess \cong J^T J + \mu I \quad (15)$$

here, the combination coefficient denoted by μ is a positive constant, and 'I' represents the identity matrix with dimensions (m × m).

By combining Eq. (7) and Eq. (15), the update value or error in measurement of the Levenberg algorithm can be presented as:

$$\delta\vec{U} = (J^T J + \mu I)^{-1} J^T \delta\vec{P}r \quad (16)$$

The combination coefficient parameter, $\mu$ changes its value adaptively and is also called an adaptive learning parameter. The implementation of the above-developed algorithm with adaptive learning parameters is discussed below.

- *Step-by-Step Computation of Navigation Solution using Levenberg method*

Step 1. Using 'm' satellites, collect pseudo-range measurements Pr1, Pr2, ..., Prm.

Step 2. Receiver position vector $\vec{U}_k = [x_{uK}, y_{uK}, z_{uK}]^T$ is initialized to 0 (i.e. K = 0), ) and combination coefficient, μ.

Step 3. Based on the receiver position in step 2, calculate the range measurements, $Pr_{1K}$ , $Pr_{2K}$, …, $Pr_{mK}$.

Step 4. Take the measurement vector $\delta\vec{P}r = [\delta Pr_1 \quad \delta Pr_2 \quad \dots \quad Pr_m]^T$ and Calculate the error from steps 1 and 3.

Step 5. Compute, $E_0 = (\delta\vec{P}r^T \; \delta\vec{P}r)$ from step 4.

Step 6. Calculate the Jacobian matrix, $J_{m\times 3}$, and the Hessian matrix, Hess=$J^T J$.

Step 7. Using Eq. (16), determine the update value or change in position $\delta\vec{U} = [\delta x_u \quad \delta y_u \quad \delta z_u]^T$

Step 8. Using the position vector obtained in Step 7, update the receiver position vector in Step 2. (i.e. $\vec{U}_{K+1} = \vec{U}_K + \delta\vec{U}$)

Step 9. Compute the range measurements, $Pr_{1K+1}$ , $Pr_{2K+1}$, …, $Pr_{mK+1}$ with the updated receiver position in step 8.

Step 10. Calculate the error in measurement vector, $\delta\vec{P}r = [\delta Pr_1 \quad \delta Pr_2 \quad \dots \quad Pr_m]^T$ from steps 1 and 9.

Step 11. Compute, $E_1 = (\delta\vec{P}r^T \; \delta\vec{P}r)$ from step 10.

Step 12. Compare $E_0$ and $E_1$: if $E_0 > E_1$ update combination coefficient using

Step 13. $\mu = \mu/10$ in Eq. (16), assign $\vec{U}_K = \vec{U}_{K+1}$, $E_0 = E_1$ and repeat steps 6 to 12. Else update combination coefficient using $\mu = \mu \times 10$ in Eq. (16) and repeat steps 7 to 12.

Step 14. Carry out iterations of Steps 6 to 12 either for a predetermined number of cycles or until the predefined threshold condition is satisfied. (like $E_0$ <= threshold).

Step 15. $\vec{U}_{K+1} = [x_{uK+1}, y_{uK+1}, z_{uK+1}]^T$ is the final receiver position estimate.

## IV. Result and Discussion

January 2014 from a dual-frequency GPS receiver located at the Indian Institute of Science (IISc) in Bangalore (lat: 13.021°N/long: 77.5°E), India. The collected GPS data is used to implement and compare the performance of the Gradient Descent with Armijo (GD with Armijo), Least Squares (LS), Weighted Least Squares (WLS), and Levenberg (LVB) algorithms. The GPS data contains two files, i.e., Navigation data and Observation data files. The observation data file is collected at a sampling rate of 30 sec throughout approximately 22 hours, while the navigation data file is for every 2 hours. Of the 36 parameters in the navigation data, only 23 are used to calculate the satellite position, angles like elevation, and azimuth. The desirable values are kept in files so that the four algorithms can estimate the receiver position and error analysis is carried out.

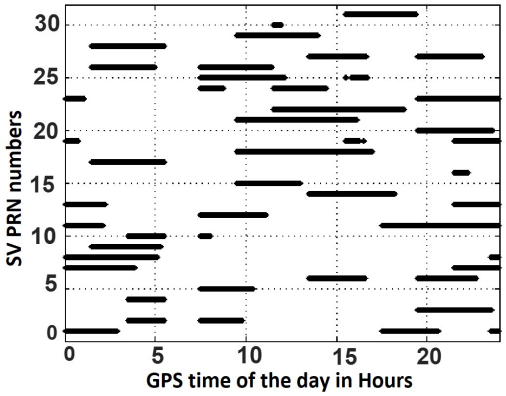


Fig. 1. Satellite visibility throughout the day on 01st January 2014.

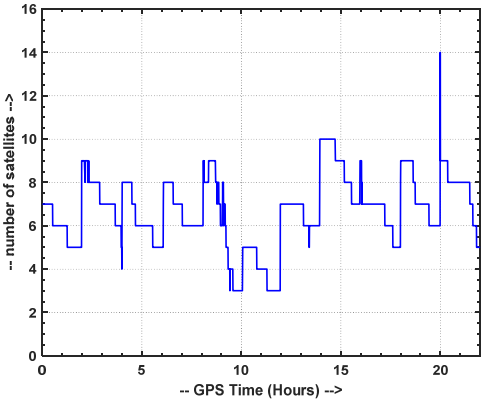


Fig. 2. Correlation between time and the number of satellites.

The IISc GPS receiver is positioned in the surveyed location, with its Earth Centered Earth Fixed (ECEF) coordinates as X = 1337936.309 m, Y = 6070317.116 m, and Z = 1427876.908 m. Fig. 1 illustrates the visibility of satellites over this region on 01st January 2014, and it can be observed that satellites with Satellite Vehicle Pseudo Random Numbers (SV PRN) 1, 2, 3, 4, 5, 6, 7, 8, 9, 10, 11, 12, 13, 14, 15, 16, 17, 18, 19, 20, 21, 22, 23, 24, 26, 27, 28, 29, 30, and 31 are visible in this location. Additionally, Fig. 2 displays the frequency of satellites for each sample throughout the day. At any given time, at least three satellites are visible near IISc, Bangalore.

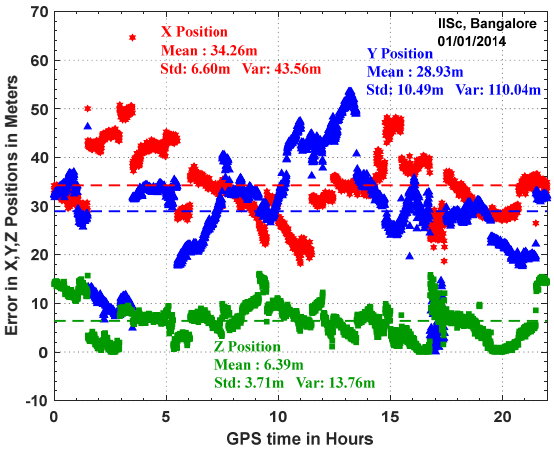


(a). using GD with Armijo

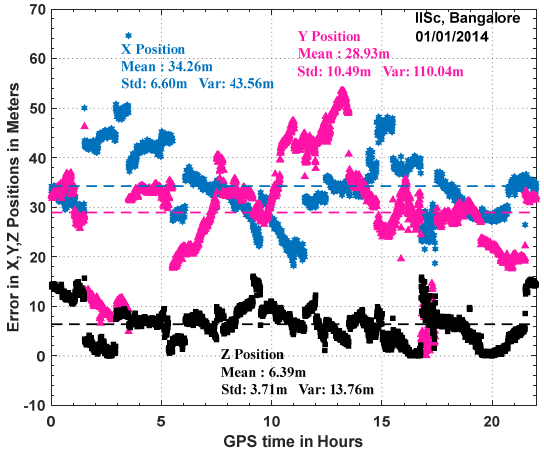


(b). using least squares

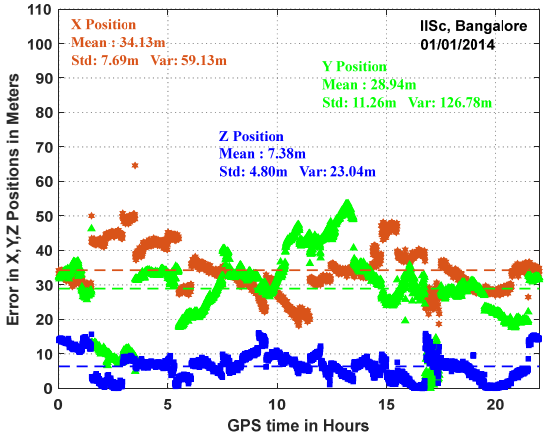


(c). using weighted least squares

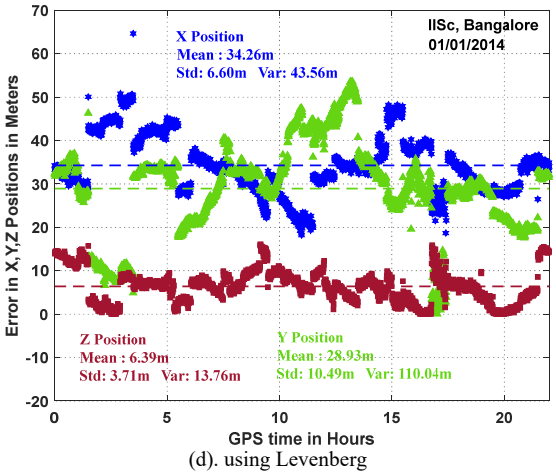


(d). using Levenberg

Fig. 3. Error in estimated position.

In addition, Fig. 3(a) to Fig. 3(d) shows that the GPS time vs. error in X, Y, and Z positions estimated using the four algorithms (i.e., Gradient Descent with Armijo, Least Squares, Weighted Least Squares, Levenberg), respectively over a day. These figures also display the corresponding mean, standard deviation, and variance values.

Likewise, the positional error resulting from the four algorithms (i.e., GD with Armijo, LS, WLS, and LVB) is also smoothened by averaging over an Hour, and Fig. 4(a) to Fig. 4(d) shows the smoothened position error. These figures also display the corresponding mean, standard deviation, and variance values.

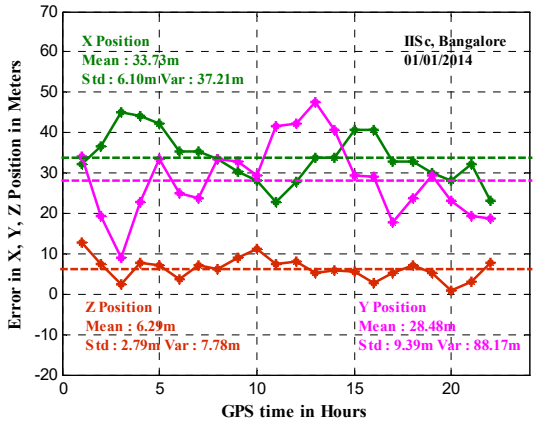


(a). using GD with Armijo

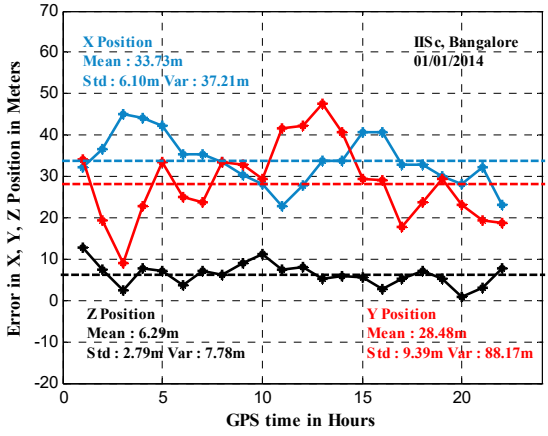


(b). using least squares

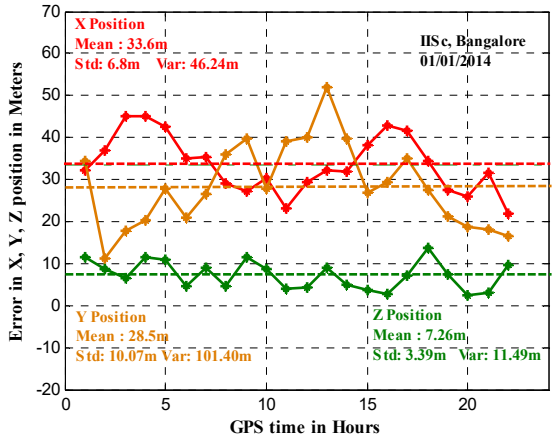


(c). using weighted least squares

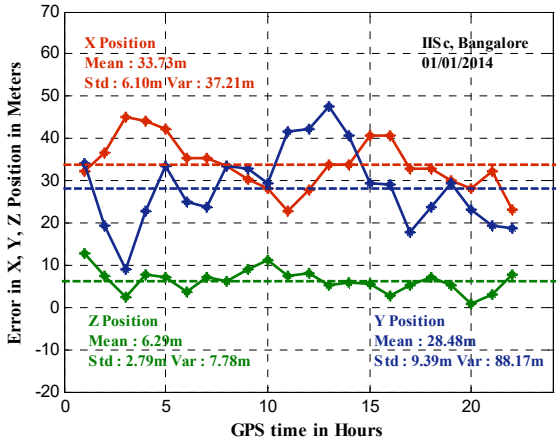


(d). using Levenberg

Fig. 4. Error in estimated position smoothened over an hour.

TABLE I. SMOOTHENED RECEIVER POSITION OVER ONE HOUR AND ASSOCIATED ERROR IN RECEIVER POSITION USING GD WITH ARMIJO (LS AND LVB)

| S.No. | GPS Time (Hours) | Receiver position (meters) | | |
|---|---|---|---|---|
| | | X | Y | Z |
| 1 | 1 | 1337904.00 | 6070282.97 | 1427864.16 |
| 2 | 2 | 1337899.70 | 6070297.67 | 1427869.53 |
| 3 | 3 | 1337891.20 | 6070308.09 | 1427874.60 |
| 4 | 4 | 1337892.15 | 6070294.20 | 1427869.27 |
| 5 | 5 | 1337893.98 | 6070283.56 | 1427869.88 |
| 6 | 6 | 1337900.90 | 6070291.96 | 1427873.12 |
| 7 | 7 | 1337900.96 | 6070293.50 | 1427869.83 |
| 8 | 8 | 1337902.73 | 6070283.68 | 1427870.66 |
| 9 | 9 | 1337906.12 | 6070284.16 | 1427867.79 |
| 10 | 10 | 1337908.10 | 6070287.58 | 1427865.70 |
| 11 | 11 | 1337913.35 | 6070275.48 | 1427869.49 |
| 12 | 12 | 1337908.51 | 6070274.79 | 1427868.98 |
| 13 | 13 | 1337902.56 | 6070269.61 | 1427871.74 |
| 14 | 14 | 1337902.38 | 6070276.39 | 1427870.96 |
| 15 | 15 | 1337895.64 | 6070287.73 | 1427871.21 |
| 16 | 16 | 1337895.68 | 6070288.10 | 1427874.24 |
| 17 | 17 | 1337903.50 | 6070299.48 | 1427871.66 |
| 18 | 18 | 1337903.43 | 6070293.47 | 1427869.94 |
| 19 | 19 | 1337906.37 | 6070287.72 | 1427871.78 |
| 20 | 20 | 1337908.16 | 6070293.86 | 1427876.11 |
| 21 | 21 | 1337904.01 | 6070297.71 | 1427873.71 |
| 22 | 22 | 1337913.31 | 6070298.29 | 1427869.08 |
| **Mean** | | 1337902.58 | 6070288.64 | 1427870.61 |
| **Standard deviation (σ)** | | 6.10 | 9.39 | 2.79 |
| **Variance ($\sigma^2$)** | | 37.25 | 88.18 | 7.81 |

TABLE II. SMOOTHENED RECEIVER POSITION ERROR OVER ONE HOUR USING GD WITH ARMIJO (LS AND LVB)

| S.No. | GPS Time (Hours) | Error (meters) | | |
|---|---|---|---|---|
| | | X | Y | Z |
| 1 | 1 | 32.31 | 34.14 | 12.75 |
| 2 | 2 | 36.61 | 19.45 | 7.38 |
| 3 | 3 | 45.11 | 9.02 | 2.31 |
| 4 | 4 | 44.16 | 22.91 | 7.64 |
| 5 | 5 | 42.33 | 33.56 | 7.02 |
| 6 | 6 | 35.41 | 25.15 | 3.79 |
| 7 | 7 | 35.35 | 23.62 | 7.08 |
| 8 | 8 | 33.58 | 33.43 | 6.25 |
| 9 | 9 | 30.19 | 32.96 | 9.12 |
| 10 | 10 | 28.21 | 29.53 | 11.21 |
| 11 | 11 | 22.96 | 41.63 | 7.41 |
| 12 | 12 | 27.80 | 42.33 | 7.92 |
| 13 | 13 | 33.75 | 47.50 | 5.17 |
| 14 | 14 | 33.93 | 40.72 | 5.95 |
| 15 | 15 | 40.67 | 29.39 | 5.70 |
| 16 | 16 | 40.63 | 29.02 | 2.67 |
| 17 | 17 | 32.81 | 17.64 | 5.25 |
| 18 | 18 | 32.88 | 23.64 | 6.97 |
| 19 | 19 | 29.94 | 29.40 | 5.13 |
| 20 | 20 | 28.15 | 23.25 | 0.80 |
| 21 | 21 | 32.30 | 19.40 | 3.20 |
| 22 | 22 | 23.00 | 18.83 | 7.83 |
| **Mean** | | 33.73 | 28.48 | 6.30 |
| **Standard deviation (σ)** | | 6.10 | 9.39 | 2.79 |
| **Variance ($\sigma^2$)** | | 37.25 | 88.18 | 7.81 |

TABLE III. SMOOTHENED RECEIVER POSITION OVER ONE HOUR IN RECEIVER POSITION USING WEIGHTED LEAST SQUARES ALGORITHM

| S.No. | GPS Time (Hours) | Receiver position (meters) | | |
|---|---|---|---|---|
| | | X | Y | Z |
| 1 | 1 | 1337904.11 | 6070282.72 | 1427865.37 |
| 2 | 2 | 1337899.49 | 6070305.95 | 1427868.15 |
| 3 | 3 | 1337891.29 | 6070299.37 | 1427870.43 |
| 4 | 4 | 1337891.21 | 6070296.88 | 1427865.47 |
| 5 | 5 | 1337893.82 | 6070289.15 | 1427866.03 |
| 6 | 6 | 1337901.25 | 6070296.13 | 1427872.30 |
| 7 | 7 | 1337901.05 | 6070290.55 | 1427867.80 |
| 8 | 8 | 1337907.29 | 6070281.18 | 1427872.35 |
| 9 | 9 | 1337909.17 | 6070277.27 | 1427865.37 |
| 10 | 10 | 1337906.10 | 6070289.25 | 1427868.26 |
| 11 | 11 | 1337913.16 | 6070278.01 | 1427873.00 |
| 12 | 12 | 1337906.93 | 6070276.92 | 1427872.46 |
| 13 | 13 | 1337903.98 | 6070265.27 | 1427867.89 |
| 14 | 14 | 1337904.42 | 6070277.51 | 1427871.95 |
| 15 | 15 | 1337898.25 | 6070290.17 | 1427873.20 |
| 16 | 16 | 1337893.36 | 6070287.84 | 1427874.06 |
| 17 | 17 | 1337894.63 | 6070282.02 | 1427869.79 |
| 18 | 18 | 1337902.02 | 6070289.55 | 1427863.11 |
| 19 | 19 | 1337908.94 | 6070295.91 | 1427869.38 |
| 20 | 20 | 1337910.21 | 6070298.48 | 1427874.60 |
| 21 | 21 | 1337904.66 | 6070298.96 | 1427874.01 |
| 22 | 22 | 1337914.38 | 6070300.54 | 1427867.18 |
| **Mean** | | 1337902.71 | 6070288.62 | 1427869.64 |
| **Standard deviation (σ)** | | 6.81 | 10.07 | 3.39 |
| **Variance ($\sigma^2$)** | | 46.37 | 101.40 | 11.49 |

It is clear from Figs. 3 and 4 that the implemented algorithms, i.e., GD with Armijo, Least Squares and Levenberg, show similar performance in position estimation. The Weighted Least squares algorithm performs differently than the above three algorithms. The following tables provide the smoothened error in position and the statistical parameters corresponding to the four

algorithms for more detailed quantitative analyses. Table I to Table IV presents the estimated receiver position coordinates (X, Y, Z) and the associated errors, mean, standard deviation, and variance for the four algorithms (GD with Armijo, LS, LVB and WLS). The results indicate that the performance of all three algorithms is comparable. The same tables also apply to the other two algorithms (LS and LVB); therefore, no separate tables are given.

TABLE IV. SMOOTHENED RECEIVER POSITION ERROR OVER ONE HOUR USING WEIGHTED LEAST SQUARES ALGORITHM

| S.No. | GPS Time (Hours) | Error (meters) | | |
|---|---|---|---|---|
| | | X | Y | Z |
| 1 | 1 | 32.20 | 34.39 | 11.54 |
| 2 | 2 | 36.82 | 11.16 | 8.76 |
| 3 | 3 | 45.02 | 17.74 | 6.48 |
| 4 | 4 | 45.10 | 20.23 | 11.43 |
| 5 | 5 | 42.49 | 27.96 | 10.88 |
| 6 | 6 | 35.06 | 20.98 | 4.61 |
| 7 | 7 | 35.26 | 26.56 | 9.10 |
| 8 | 8 | 29.02 | 35.94 | 4.56 |
| 9 | 9 | 27.14 | 39.85 | 11.54 |
| 10 | 10 | 30.21 | 27.86 | 8.65 |
| 11 | 11 | 23.15 | 39.11 | 3.91 |
| 12 | 12 | 29.38 | 40.19 | 4.45 |
| 13 | 13 | 32.33 | 51.84 | 9.02 |
| 14 | 14 | 31.89 | 39.60 | 4.96 |
| 15 | 15 | 38.06 | 26.95 | 3.70 |
| 16 | 16 | 42.95 | 29.28 | 2.85 |
| 17 | 17 | 41.68 | 35.10 | 7.12 |
| 18 | 18 | 34.29 | 27.56 | 13.80 |
| 19 | 19 | 27.37 | 21.21 | 7.53 |
| 20 | 20 | 26.10 | 18.63 | 2.31 |
| 21 | 21 | 31.65 | 18.16 | 2.90 |
| 22 | 22 | 21.93 | 16.58 | 9.72 |
| **Mean** | | 33.60 | 28.50 | 7.27 |
| **Standard deviation (σ)** | | 6.81 | 10.07 | 3.39 |
| **Variance ($\sigma^2$)** | | 46.37 | 101.40 | 11.49 |

From Table I to Table IV, the mean error in the estimated position and uncertainty in the estimation observed for both the receivers are as follows:

1. The mean position errors due to GD with Armijo, LS and LVB algorithms are $X$ = 33.73 m, $Y$ = 28.48 m, and $Z$ = 6.30 m. The corresponding uncertainties observed are $\sigma_x$ = 6.10 m, $\sigma_y$ = 9.39 m, and $\sigma_z$ = 2.79 m, respectively.
2. The mean position errors due to the WLS algorithm are $X$ = 33.60 m, $Y$ = 28.50 m, and $Z$ = 7.27 m. The corresponding uncertainties observed are $\sigma_x$ = 6.81 m, $\sigma_y$ = 10.07 m, and $\sigma_z$ = 3.39 m, respectively.

Based on the two observations mentioned earlier, it is evident that the receiver position estimates exhibit lower errors and reduced uncertainty in their estimations.

To evaluate the performance of these four algorithms, the error analysis values for all four methods are depicted in Table V, and the performance of these algorithms in terms of an average number of iterations required for position convergence with smoothened data over an Hour is given in Table VI.

It is observed from Table V the accuracy in position estimation with WLS shows a slight change over the other three algorithms with a difference in position error mean of $X$ = −0.13 m, $Y$ = 0.02 m and $Z$ = 0.97 m. It is also seen from Table III that the uncertainty in the estimated position with WLS has shown a variation in the performance change over the other three algorithms with $\sigma_x$ = 0.71 m, $\sigma_y$ = 0.68 m, $\sigma_z$ = 0.6 m for low noisy measurements (which shows degraded two dimensional and three-dimensional position accuracy). This shows that the weighted least squares perform poorly compared to the other algorithms.

From Table VI, the convergence time (number of iterations) corresponding to the four algorithms demonstrates that the LS algorithm takes 5 to 6 iterations to converge depending on the available number of satellites at that specific time. While LVB takes a negligible amount of time greater than LS (i.e., 6 to 7 iterations), WLS and GD with Armijo take the maximum time with a minimum of 31 and 59 iterations for convergence, respectively. From Tables V and VI, LS and LVB algorithms provide accurate position estimates within the acceptable time for real-time precise GPS applications.

TABLE V. COMPARISON OF STATISTICAL ERROR CHARACTERISTICS PERFORMANCE DUE TO FOUR METHODS

| Error parameter | GD with Armijo, LS and LVB | | | WLS | | |
|---|---|---|---|---|---|---|
| | X | Y | Z | X | Y | Z |
| Min | 22.95 | 9.02 | 0.79 | 21.93 | 11.16 | 2.31 |
| Max | 45.10 | 47.50 | 12.74 | 45.10 | 51.84 | 13.80 |
| μ | 33.73 | 28.48 | 6.30 | 33.60 | 28.50 | 7.27 |
| σ | 6.10 | 9.39 | 2.79 | 6.81 | 10.07 | 3.39 |
| $\sigma^2$ | 37.21 | 88.17 | 7.78 | 46.37 | 101.4 | 11.49 |

* μ- Mean, σ- Standard deviation, $\sigma^2$-Variance

TABLE VI. COMPARISON OF ITERATIONS/EPOCH FOR THE DATA SMOOTHENED OVER AN HOUR

| S. No. | GPS time (Hours) | GD with Armijo | LS | WLS | LVB |
|---|---|---|---|---|---|
| 1 | 1 | 34 | 5 | 48 | 6 |
| 2 | 2 | 34 | 6 | 49 | 6 |
| 3 | 3 | 31 | 5 | 49 | 6 |
| 4 | 4 | 37 | 5 | 49 | 6 |
| 5 | 5 | 38 | 5 | 49 | 6 |
| 6 | 6 | 48 | 5 | 49 | 7 |
| 7 | 7 | 39 | 5 | 49 | 6 |
| 8 | 8 | 37 | 5 | 48 | 6 |
| 9 | 9 | 35 | 6 | 49 | 6 |
| 10 | 10 | 63 | 6 | 39 | 7 |
| 11 | 11 | 36 | 6 | 47 | 7 |
| 12 | 12 | 386 | 6 | 49 | 8 |
| 13 | 13 | 33 | 6 | 49 | 6 |
| 14 | 14 | 40 | 5 | 49 | 6 |
| 15 | 15 | 45 | 5 | 49 | 6 |
| 16 | 16 | 51 | 5 | 50 | 7 |
| 17 | 17 | 48 | 6 | 49 | 7 |
| 18 | 18 | 64 | 5 | 49 | 7 |
| 19 | 19 | 38 | 5 | 50 | 6 |
| 20 | 20 | 39 | 5 | 49 | 6 |
| 21 | 21 | 41 | 5 | 49 | 6 |
| 22 | 22 | 40 | 6 | 49 | 6 |
| **Minimum** | | 31 | 5 | 39 | 6 |
| **Maximum** | | 386 | 6 | 50 | 7 |
| **Total** | | 1257 | 118 | 1066 | 139 |

### *A. Benchmarking*

To evaluate the effectiveness of the proposed Levenberg (LVB) algorithm, we conducted a comprehensive

benchmarking analysis against the Least Squares (LS) algorithm. The results of this analysis are detailed in Table VII. We compared these algorithms based on their positional accuracy and computational efficiency.

TABLE VII. RECEIVER POSITION ESTIMATION WITH LS AND LVB FOR THREE SATELLITE VISIBILITY

| Configuration no. | Satellite coordinates in meters (ECEF-cartesian representation) | | | Error in position (in meters) | | | |
|---|---|---|---|---|---|---|---|
| | x | y | z | Least Squares (LS) | Levenberg (LVB) | | |
| 1 | 14161180.72 | 17717961.24 | −13972022.12 | Singular matrix -inverse problem | 81.54 | 47.65 | 35.36 |
| | −7075137.32 | 20439965.20 | −15125427.30 | | | | |
| | −7075137.32 | 20439965.20 | −15125427.30 | | | | |
| 2 | 14161180.72 | 17717961.24 | −13972022.12 | | 111.50 | 1.14 | 23.41 |
| | −1375856.27 | 25740815.69 | −4723282.56 | | | | |
| | V1375856.27 | 25740815.69 | −4723282.56 | | | | |
| 3 | 14161180.72 | 17717961.24 | −13972022.12 | | 108.26 | 0.88 | 20.91 |
| | 1032530.24 | 25974108.88 | −5566840.62 | | | | |
| | 1032530.24 | 25974108.88 | −5566840.62 | | | | |
| 4 | 14161180.72 | 17717961.24 | −13972022.12 | | 48.77 | 3.49 | 25.33 |
| | 5931617.34 | 17066515.77 | 19789697.55 | | | | |
| | 5931617.34 | 17066515.77 | 19789697.55 | | | | |
| 5 | 6456138.12 | 25564621.82 | −2047082.71 | | 73.42 | 96.17 | 81.60 |
| | −7075137.32 | 20439965.20 | −15125427.30 | | | | |
| | −7075137.32 | 20439965.20 | −15125427.30 | | | | |

The LS algorithm, while computationally intensive due to Hessian matrix calculations, occasionally faced divergence issues. In contrast, the LVB algorithm, by incorporating features from both GD and LS and using an adaptive learning coefficient, provided more accurate and reliable position estimates without the inversion issues encountered in LS. The benchmarking results indicated that the LVB algorithm outperforms the traditional methods, offering lower positional errors and improved stability, even in conditions of low satellite visibility. This demonstrates the potential of the LVB algorithm to enhance GPS positioning accuracy for users in the Indian subcontinent.

## V. CONCLUSION

This paper introduces LVB, a novel navigation solution evaluated against traditional methods (GD, LS, WLS) using GPS receiver data from southern India. GD's Armijo step-length induces oscillations, prolonging convergence, while LS faces complexity with the Hessian matrix, prone to divergence. WLS's weight matrix estimation adds complexity and unpredictability. In contrast, LVB combines GD's adaptive learning with LS's stability, offering superior GPS accuracy even in low satellite visibility across the Indian subcontinent.

## CONFLICS OF INTEREST

The authors declare no conflict of interest.

## AUTHOR CONTRIBUTIONS

Dr. L. Ganesh provided the dataset crucial for the study, enabling a comprehensive analysis and ensuring the robustness of the research findings; Dr. P. Sirish Kumar and Dr. V. B. S. Srilatha Indira Dutt co-wrote the manuscript and played a significant role in shaping the overall direction and planning of the study. Their collaborative efforts ensured a cohesive and well-structured presentation of the research; Dr. A. Jayalaxmi, P. Krishna Rao, and Dr. P. Kameswara Rao participated in drafting the manuscript and provided critical revisions, enhancing the clarity and quality of the final document. All authors had approved the final version

## REFERENCES


[1] Kumar, P. Sirish, and VBS Srilatha Indira Dutt, "The global positioning system: Popular accuracy measures," *Materials today: proceedings,* vol. 33, no. 7, pp. 4797-4801, 2020.

[2] T. Liu *et al.*, "Characteristics of phase bias from CNES and its application in multi-frequency and multi-GNSS precise point positioning with ambiguity resolution," *GPS Solutions,* vol. 25, no. 2, pp. 1–13, 2021.

[3] L. Zhou, J. Shi, and D. Yang, "Vehicle positioning monitoring system based on GPS/BDS dual-mode positioning technology," in *Proc. 2024 IEEE 4th International Conference on Electronic Technology, Communication and Information (ICETCI)*, Changchun, China, 2024, pp. 704–710. doi: 10.1109/ICETCI61221.2024.10594201, 2024

[4] P. S. Kumar and VBS S. I. Dutt. "The global positioning system: Popular accuracy measures," *Materials Today: Proceedings*, vol. 33, pp. 4797–4801, 2020.

[5] R. Sun, Z. Zhang, Q. Cheng, and W. Y. Ochieng, "Pseudorange error prediction for adaptive tightly coupled GNSS/IMU navigation in urban areas," *GPS Solut.*, vol. 26, no. 1, pp. 1–13, Dec. 2022.

[6] D. Davide, E. Falletti, and M. Luise, *Satellite and Terrestrial Radio Positioning Techniques: A Signal Processing Perspective*, Academic Press, 2012.

[7] P. Horejsi, T. Machac, and M. Simon, "Reliability and accuracy of indoor warehouse navigation using augmented reality," *IEEE Access*, vol. 12, pp. 94506–94519. doi: 10.1109/ACCESS.2024.3420732, 2024

[8] D. Borio and C. Gioia. "GNSS interference mitigation: A measurement and position domain assessment," *NAVIGATION, Journal of the Institute of Navigation*, vol. 68, no. 1, pp. 93–114, 2021.

[9] H. S. Lee *et al.*, "Regional GPS orbit determination using code-based pseudorange measurement with residual correction model," *Journal of Applied Geodesy*, vol. 18, no.3, pp. 375–389, 2024.

[10] M. Peretic and G. X. Gao, "Design of a parallelized direct position estimation-based GNSS receiver Navigation," *NAVIGATION: Journal of the Institute of Navigation*, vol. 68, no. 1, pp. 21–39, 2021.

[11] N. Z. Jhanjhi, L. Gaur, and N. A. Khan, "Global navigation satellite systems for logistics," *Cybersecurity in the Transportation Industry*, pp. 49–67, 2024. doi: 10.1002/9781394204472

[12] N. A. Kumar *et al.*, "Development of a double resampling based least-squares particle filter for accurate position estimation of a GPS

receiver in Visakhapatnam region of the Indian subcontinent," *IEEE Sensors Journal*, vol. 24, no. 5, pp. 5539–5548, 2023.
[13] J. Zhang and W. Li. "Analysis of post-processed pseudorange-based point positioning with different data sources for the current galileo constellations," *Sensors*, vol. 24, no. 8, pp. 2472, 2024.
[14] F. Zhou and X. Wang, "Some key issues on pseudorange-based point positioning with GPS, BDS-3, and galileo observations," *Remote Sensing*, vol. 15, no. 3 p. 797, 2023.
[15] V. Buren, Damon, P. Axelrad, and S. Palo. "A low complexity smoothing algorithm for improved GPS point solutions on board LEO spacecraft." *NAVIGATION: Journal of the Institute of Navigation*, vol. 68, no. 1, pp. 185–198, 2021.
[16] Y. Zhu, Y. Ma, X. Chen, Y. Yang and S. Yang, "Comparison of radiated A-GNSS sensitivity measurement and stand-alone GNSS tracking sensitivity measurement," in *Proc. 2024 IEEE International Workshop on Radio Frequency and Antenna Technologies (iWRF&AT)*, Shenzhen, China, 2024, pp. 173–175. doi: 10.1109/iWRFAT61200.2024.10594493
[17] Kumar, P. Sirish, and VBS S. I. Dutt. "Evaluation of GPS receiver position accuracy improvement using least squares estimator over the south zone of Indian subcontinent," *Jour. of Adv. Research in Dynamical & Control Systems*, vol. 11, no. 6, pp. 114–119, 2019.
[18] X. Zhang, Y. Zhang, and F. Zhu, "A method of improving ambiguity fixing rate for post-processing kinematic GNSS data," *Satellite Navigation*, vol. 1, no. 1, pp. 1–13, 2020.
[19] Z. Zhang, X. Lian and W. Sun, "Towards seamless localization in challenging environments via high-definition maps and multi-sensor fusions," in *Proc. 2024 IEEE Intelligent Vehicles Symposium (IV)*, Jeju Island, Korea, 2024, pp. 933–940. doi: 10.1109/IV55156.2024.10588504
[20] R. Sun, L. Fu, Q. Cheng, K. -W. Chiang and W. Chen, "Resilient pseudorange error prediction and correction for GNSS positioning in urban areas," *IEEE Internet of Things Journal*, vol. 10, no. 11, pp. 9979–9988, 2023. doi: 10.1109/JIOT.2023.3235483

Copyright © 2024 by the authors. This is an open access article distributed under the Creative Commons Attribution License (CC BY-NC-ND 4.0), which permits use, distribution and reproduction in any medium, provided that the article is properly cited, the use is non-commercial and no modifications or adaptations are made.